Evolution of skull and body shape in Triturus newts reconstructed from three-dimensional morphometric data and phylogeny

Ana Ivanović , Jan W. Arntzen

The LINNEAN SOCIETY of London BIOLOGICAL Journal of the Linnean Society

Biological Journal of the Linnean Society, 2014, **113**, 243–255. With 6 figures

Evolution of skull and body shape in *Triturus* newts reconstructed from three-dimensional morphometric data and phylogeny

ANA IVANOVIĆ[1,2]* and JAN W. ARNTZEN[2]

[1]*Faculty of Biology, Institute for Zoology, University of Belgrade, Studentski trg 16, 11000 Belgrade, Serbia*
[2]*Naturalis Biodiversity Center, PO Box 9517, 2300 RA Leiden, The Netherlands*

Received 12 February 2014; revised 4 March 2014; accepted for publication 4 March 2014

To explore the relationship between morphological change and species diversification, we reconstructed the evolutionary changes in skull size, skull shape, and body elongation in a monophyletic group of eight species that make up salamander genus *Triturus*. Their well-studied phylogenetic relationships and the marked difference in ecological preferences among five species groups makes this genus an excellent model system for the study of morphological evolution. The study involved three-dimensional imagery of the skull and the number of trunk vertebrae, in material that represents the morphological, spatial, and molecular diversity of the genus. Morphological change largely followed the pattern of descent. The reconstruction of ancestral skull shape indicated that morphological change was mostly confined to two episodes, corresponding to the ancestral lineage that all crested newts have in common and the *Triturus dobrogicus* lineage. When corrected for common descent, evolution of skull shape was correlated to change in skull size. Also, skull size and shape, as well as body shape, as inferred from the number of trunk vertebrae, were correlated, indicating a marked impact of species' ecological preferences on morphological evolution, accompanied by a series of niche shifts, with the most pronounced one in the *T. dobrogicus* lineage. The presence of phylogenetic signal and correlated evolutionary changes in skull and body shape suggested complex interplay of niche shifts, natural selection, and constraints by a common developmental system. *Biological Journal of the Linnean Society*, 2014, **113**, 243–255.

ADDITIONAL KEYWORDS: Caudata – cranium – geometric morphometric – micro CT-scan – Salamandridae – vertebrae number.

INTRODUCTION

Variation in organismal size and shape is generally assumed to be adaptive, and thus shaped by natural selection. However, a shared developmental system inherited from a common ancestor, as well as structural and functional requirements, can restrict the response to selection (Lande & Arnold, 1983; Richardson & Chipman, 2003; Wagner & Mezey, 2004; Galis & Metz, 2007). Accordingly, the similarity of organisms could result from living in similar environments, from structural and functional constraints, and from a shared evolutionary history (Gould, 2002; Blomberg, Garland & Ives, 2003; Losos, 2011) and an independently derived phylogeny is required to disentangle the effects of these influences. Although the importance of 'the comparative method' is well established (Felsenstein, 1985; Harvey & Pagel, 1991; Brooks *et al*., 1995), empirical studies that explore the relationship between covariation in geometric morphometric data and phylogeny, with reference to species' ecological preferences and the environment, are scarce (Cardini & Elton, 2008a; Adams & Nistri, 2010; Perez *et al*., 2011; Álvarez, Perez & Verzi, 2013).

We studied morphology and descent in a group of ecologically differentiated species in the old (approximately 24 Mya; Steinfartz *et al*., 2007) and monophyletic group of large-bodied newts (genus *Triturus*, family Salamandridae). Species' ecological preferences (from predominantly terrestrial to largely aquatic) coincide with five morphotypes that form a series from short and stout to elongated and slender

*Corresponding author. E-mail: ana@bio.bg.ac.rs

(Arntzen, 2003). These morphotypes are originally defined by the forelimb to interlimb ratio, known as the Wolterstorff index (Wolterstorff, 1923; Arntzen & Wallis, 1994) and are characterized by a particular number of trunk vertebrae [or number of rib-bearing vertebrae (NRBV)]. The morphological–ecological series across the eight species is: (1) *Triturus marmoratus* and *Triturus pygmaeus* (NRBV 12; 2 months in water); (2) *Triturus ivanbureschi* and *Triturus karelinii* (NRBV 13; three months in water); (3) *Triturus carnifex* and *Triturus macedonicus* (NRBV 14; 4 months in water); (4) *Triturus cristatus* (NRBV 15; 5 months in water); and (5) *Triturus dobrogicus* (NRBV 16–17; 6 months in water). In particular, Arntzen & Wallis (1999) hypothesized that body elongation as seen in the genus *Triturus* is an adaptation that allows better locomotor performance in water. This hypothesis is strongly supported by the association of NRBV and annual time spent in water. Concordance between length of aquatic period and body elongation suggests that morphological diversification in *Triturus* newts emerged from a change in ecological preferences and renders the group as a model for evolutionary studies at the interface of morphology and ecology.

To estimate the significance of external factors (ecological parameters and natural selection) and internal factors (developmental and functional constraints) on the morphological evolution of *Triturus* newts, we selected two, functionally unrelated complex morphological traits, namely skull form (size and shape) and axial skeleton (body shape). The cranium and the axial skeleton have largely decoupled developmental pathways. Most of the cranial skeletal elements derive from the streams of neural crest cells, whereas the axial skeleton derives from the segmented mesoderm (i.e. somites). The exception is the otico-occipital unit of the skull, which derives from the first somites and the paraxial mesoderm (Hall, 2003).

In the present study, we aimed to: (1) document intra- and inter-specific morphological variation in these traits in *Triturus* salamanders; (2) analyze this variation in a phylogenetic context; and (3) explore the data for co-evolutionary change. Additionally, we explored the possible developmental modularity of the cranial skeleton (derived from the neural crest versus the otico-occipital unit), also in the phylogenetic context.

MATERIAL AND METHODS

Phylogenetic analysis

As a temporal framework for our analyses, we reconstructed a calibrated phylogeny of the family Salamandridae, from which we lifted the *Calotriton–Triturus* clade. This top-down approach was taken because convincing fossil data for the genus *Triturus* are rare, whereas some are available for the Salamandridae as a whole. Altogether, dating of the phylogeny was based upon a wide range of temporal calibration points provided by seven fossils, *sensu* Wiens, Sparreboom & Arntzen (2011).

The phylogeny of the family Salamandridae was estimated from 50 published sequences of the full mitochondrial genome, representing 42 salamandrid species and four outgroups (*Ambystoma mexicanum*, *Andrias davidianus*, *Ranodon sibiricus*, and *Rhyacotriton variegatus*, Zhang *et al*., 2008; Wielstra & Arntzen, 2011). The data can be found at the TreeBase repository under numbers S9945 and S11081. We performed a combined phylogeny and divergence-time estimation using the Bayesian uncorrelated lognormal approach (Drummond *et al*., 2006) implemented in BEAST, version 1.5.4 (Drummond & Rambaut, 2007) and the results were analyzed and presented with associated software (LOGCOMBINER, TREEANNOTATOR, FIGTREE and TRACER at http://beast.bio.ed.ac.uk).

BEAST analyses were conducted with separate partitions for different codon positions in 13 coding genes and other partitions for 12S, 16S, and the combined RNAs (with rate parameters, rate heterogeneity, and base frequencies unlinked across partitions but with clock and tree models linked), with estimated base frequencies, and with trees generated using a Yule speciation process and with nucleotide substitution models suggested by MRMODELTEST (Nylander, 2004). We ran three replicate analyses of 100 million and two of 200 million generations of which the initial 90% of each run were excluded as burn-in. All five runs yielded effective sample sizes > 200 for likelihood and ages of the majority of clades as shown with TRACER. For analyses of character evolution, we used the maximum clade-credibility tree from the combined results of the five runs, using mean clade heights for clade ages, retrieved and represented with LOGCOMBINER, TREEANNOTATOR and FIGTREE.

Sampling and morphology

Three-dimensional (3D) models of *Triturus* skulls were obtained from 177 specimens (121 cleared and stained skeletons from the Institute of Biological Research 'Siniša Stanković', Belgrade, and 56 alcohol preserved at the Naturalis Biodiversity Center, Leiden). The NRBV was counted in 144 cleared and stained skeletons and from X-ray imagery of 39 alcohol preserved specimens. Body elongation by an increase in the number of vertebrae is common in salamanders, whereas body elongation through lengthening of vertebrae without a change in the number is only known

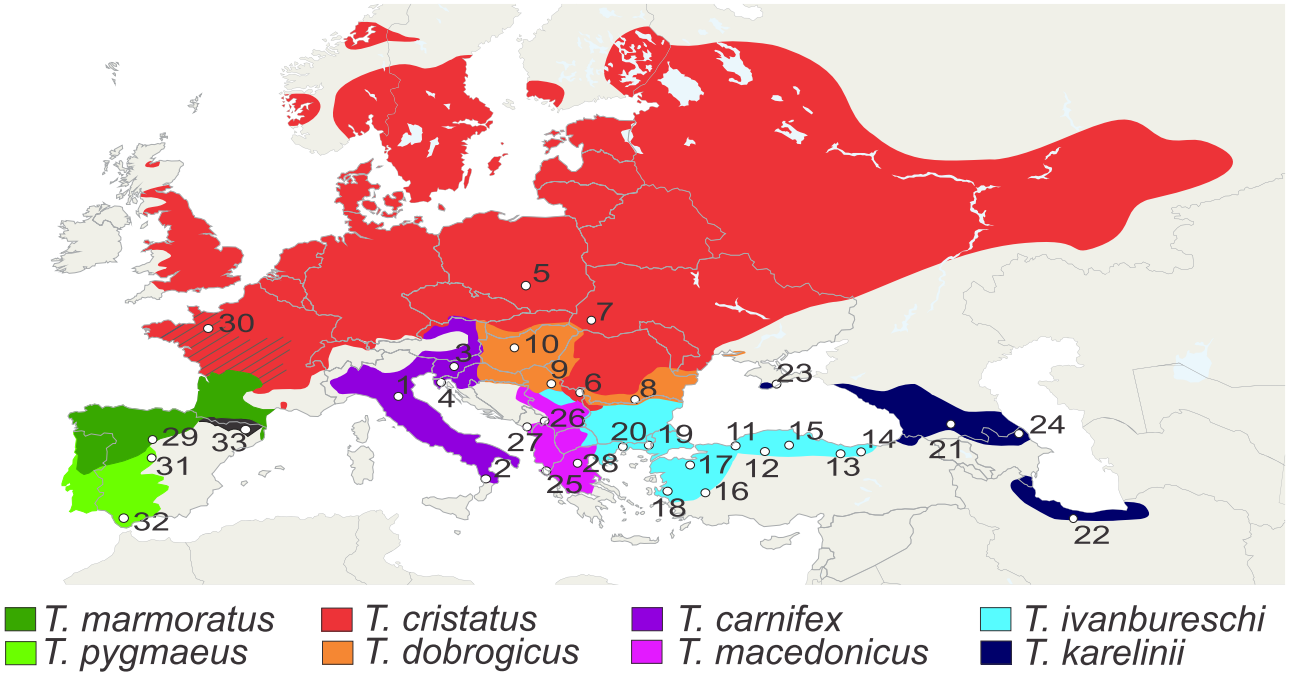

Figure 1. Distribution of eight *Triturus* species across Europe and adjacent Asia. The outgroup *Calotriton asper* from the Pyrenees is shown in black. Studied populationms are marked by numbers. For detailed information, see Supporting information (Table S1).

for *Pseudoeurycea lineola* (Wake, 1991; Parra-Olea & Wake, 2001). To avoid confounding effects from sexual dimorphism (Arntzen, 2000; Ivanović & Kalezić, 2012), analyses of the skull were, with few exceptions, limited to the female sex (see Supporting information, Table S1; note that no marked sexual dimorphism is present in NRBV). Our material covers geographical, taxonomic, and molecular genetic diversity of the genus (Fig. 1; see also Supporting information, Table S1). Sample size per species ranged from 10–55 (mean 21.1) for the skull and from 10–65 (mean 22.4) for NRBV. For comparison, we included two males and four females of *Calotriton asper* because this species represents the sister group (and thus nearest outgroup) of the genus *Triturus* (Steinfartz *et al*., 2007).

Selected specimens were scanned with a Skyscan 1172 100 kV computed microtomograph [micro computed tomography (CT)-scanner] under settings that were optimized for the material (aluminium filter 0.5 mm, 74 kV, 0.8 rotation step, 515 ms exposure time, four frame averaging). Flat field corrections were performed automatically. At the two-dimensional (2D) reconstruction stage, global threshold values were verified manually. 3D surface models of newt skulls were produced using SkyScan CT ANALYSER, version 1.10 software, under a marching cube algorithm and a resolution of 26.1 μm. Further analysis was based on 3D landmark configurations obtained directly from the corresponding surface models. Forty-eight landmarks were defined of which four were median landmarks and 22 were bilaterally symmetric landmarks. The landmarks represent clearly distinguishable anatomical positions, are more or less evenly distributed over the skull and thus represent the skull entirely. A key to the landmarks, brief anatomical descriptions, and partition of the landmarks into subsets corresponding to their origin (the neural crest versus the otico-occipital unit) is provided in Figure 2 (see also Supporting information, Table S2). The landmark coordinates were recorded from the surface models using LANDMARK IDAV, version 3.0 (http://graphics.idav.ucdavis.edu/research/EvoMorph).

Skull size was computed as the centroid size (CS, the measure of size in geometric morphometrics) and reflects the amount of dispersion around the centroid of the landmark configuration. We applied a generalized Procrustes analysis (Rohlf & Slice, 1990; Dryden & Mardia, 1998) to obtain a matrix of shape coordinates (the so-called Procrustes coordinates) that is free of differences as a result of position, scale, and orientation. Having digitized landmarks on both sides of the skull, we mirrored and averaged the bilaterally symmetric landmarks to remove the redundancy of bilaterally homologous landmarks (Klingenberg, Barluenga & Meyer, 2002). To reduce the dimensionality of the data, we carried out a multivariate ordination by a principal component analysis (PCA), based on the covariance matrix.

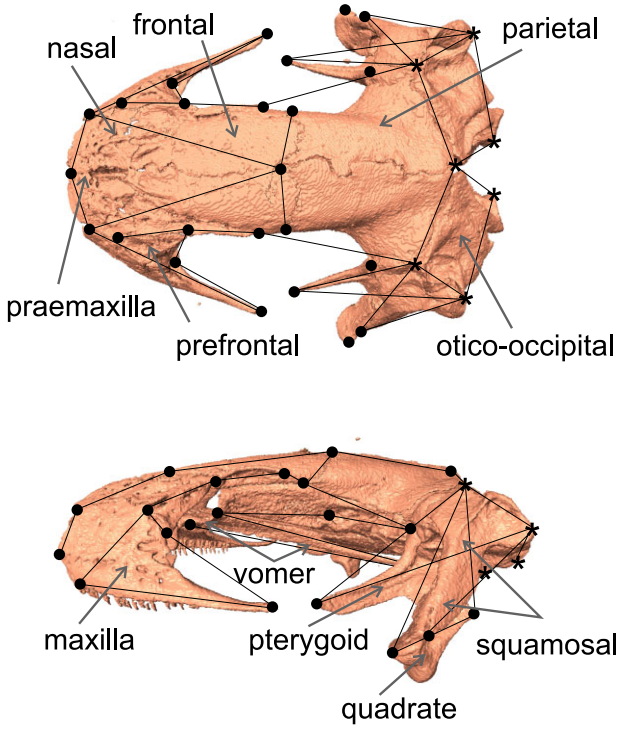

Figure 2. Landmarks and wireframe superimposed on the dorsal and lateral side of a token *Triturus* skull. The image of the skull is derived from a computed tomography scan with a spatial resolution of 26.1 μm. The partition of the landmarks into subsets corresponding to the hypothesized modules is shown as: neural crest origin (solid circles) and otico-occipital region (asterisks). For the description of landmarks, see Supporting information (Table S2).

The effects of species on size (CS) and on skull shape (PCA scores) were tested with analysis of variance (ANOVA) and multivariate analysis of variance (MANOVA), respectively. The statistical significance of difference in skull size between species was tested with Tukey's honestly significant difference post-hoc test in SAS, version 9.1.3 (SAS Institute Inc.). To quantify the shape differences, we used Procrustes distances for each pair of species. The statistical significance of differences in mean shape between species was estimated by permutation test based on 10 000 iterations using MORPHOJ (Klingenberg, 2011) and interpreted under Bonferroni correction. Differences among species in skull shape were also explored with a discriminant function analysis and we report the original and cross-validation results as the percentage of cases correctly classified. For cross-validation, we applied the leave-one-out cross-validation test, which uses a single observation from the original sample as validation. The comparison of both percentages quantifies the uncertainty in assigning individuals to groups (Manly, 1997).

Phylogenetic signal and character reconstruction

Associations derived from common ancestry were evaluated by calculating the strength of the phylogenetic signal (for skull size, skull shape, and body shape), which we tested for statistical significance using MORPHOJ (Klingenberg, 2011). The procedure involves random permutation of the landmark configurations over the terminal units of the phylogenetic tree (10 000 iterations), in which the test statistic is the total amount of squared change summed over all branches of the tree. Character states for the internal nodes were estimated from the mean values for terminal units under the criterion of squared-change parsimony, weighted by the amount of molecular change over the respective branches of the tree (Maddison, 1991; McArdle & Rodrigo, 1994; Rohlf, 2001).

To visualize the evolutionary history of skull shape in *Triturus*, we projected the phylogenetic tree into morphometric space defined by first and second PCs, which was then superimposed on the estimated time scale, to visualize the evolution of skull shape over time. This 'chrono-phylo-morphospace' representation of skull shape evolution was made with the PHYTOOLS and GEIGER packages in R (Harmon *et al.*, 2008; Revell, 2012). To reconstruct/estimate values for the internal nodes, the generalized least squares method was used, such that the sum of squared changes along the branches is minimized over the entire phylogeny (Klingenberg & Gidaszewski, 2010).

To investigate the changes that account for most of the evolutionary differentiation along the branches of the tree, we conducted the PCA on reconstructed shape changes along branches of a tree. As the starting dataset, we used the changes along all branches in the phylogeny that were weighted by branch length. In the space defined with PC axes, points represent change of skull shape along the specific branches (Klingenberg, 2011).

We used the phylogenetic independent contrasts approach (Felsenstein, 1985) to obtain a set of independent contrasts of skull shape, skull size, and NRBV. Subsequently, the contrast for shape was regressed on those for NRBV and size, which allowed an exploration of the association of these traits with similarity as a result of shared ancestry accounted for. Statistical significance of regression was tested with a permutation test (10 000 iterations) against the null hypothesis of random distribution. The independent contrast analyses and the regression analyses were carried out using MORPHOJ.

We evaluated the hypothesis of evolutionary modularity of the otico-occipital region and the neural

crest-derived part of the skull by comparing covariation between these two pre-defined modules, with covariation between the randomly partitioned set of landmarks, *sensu* Klingenberg (2009). A connectivity graph was used for defining the spatial contingency of the modules. Spatial contingency is achieved if every landmark in the set is connected to every other landmark in the set, either directly, or indirectly through other landmarks of the same set. The strength of covariation between two sets of landmarks is quantified with the coefficient RV. RV runs from zero to unity and describes the strength of association between the sets of landmarks. The significance level of the test is the proportion of cases in which the RV coefficient computed for randomly partitioned sets matches or exceeds the value obtained from the hypothetized partition (10 000 iterations). To test the modularity hypothesis, we used the independent contrast dataset. Because independent contrasts are shape changes (not actual shapes), they cannot be used directly in the Procrustes superimposition (Klingenberg & Marugán-Lobón, 2013). Instead, the mean shape was added to the vectors of independent contrasts as implemented in MORPHOJ (Klingenberg, 2011).

RESULTS

Phylogenetic analysis

A time-calibrated phylogeny for the *Calotriton–Triturus* clade is presented in the Supporting information (Fig. S1). Bayesian posterior probabilities are at unity for all branches. Ages associated with species diversification are 36.9 Mya for node 1, 25.0 Mya for node 2, 9.4 Mya for node 3, 8.1 Mya for node 4, 7.4 Mya for node 5, 7.4 Mya for node 6, 5.2 Mya for node 7, and 4.7 Mya for node 8 (see Supporting information, Fig. S1). In summary, the basal split between the marbled newts (*T. marmoratus* and *T. pygmaeus*) and the crested newts (*T. ivanbureschi*, *T. karelinii*, *T. carnifex*, *T. macedonicus*, *T. cristatus*, and *T. dobrogicus*) was estimated at 25.0 Mya and the further diversification was at 5–10 Mya.

Morphological divergences

We found that *Triturus* species significantly differ in skull size (ANOVA, $SS = 0.0016$, model d.f. = 7, error d.f. = 163, $F = 32.20$, $P < 0.0001$). The number of rib-bearing vertebrae observed in the eight *Triturus* species is given in the Supporting information (Table S1). The modal numbers are as reported previously (Arntzen, 2003; Wielstra & Arntzen, 2011; Ivanović *et al.*, 2013), except for *T. dobrogicus*, which had approximately equal numbers for the NRBV = 16 and NRBV = 17 classes. For the analyses, we use the lower number.

The mean skull sizes (CS) are given in the Supporting information (Table S3). Pairwise comparisons indicated that skull size in *T. dobrogicus* is smaller than in all other species and that the skulls of *T. cristatus* and *T. pygmaeus* are smaller than that of most other species (Table 1; see also Supporting information, Table S3).

From the 70 PC axes in the covariance matrix (see Supporting information, Table S4), axes 1–23 together describe > 90% of the observed variance in skull shape, and were used as dependent variables in MANOVA test. Differences in skull shape among the taxa are highly significant (MANOVA, Wilks' lambda = 1.22×10^{-4}, $F = 16.80$, $\text{d.f.}_1 = 161$, $\text{d.f.}_2 = 959.57$, $P < 0.0001$) and also the skull mean shape was significantly different in all pairwise comparisons (Table 1).

Table 1. Difference in skull size and skull shape between species of *Triturus* newts, and the correct classification of individuals to the species based on skull shape summarized from pairwise discriminant function analyses

Species	1	2	3	4	5	6	7	8
1 *Triturus carnifex*		**0.051**	**0.085**	**0.040**	**0.049**	**0.043**	**0.084**	**0.068**
2 *Triturus cristatus*	**3.6**		**0.062**	**0.054**	**0.060**	**0.058**	**0.092**	**0.079**
3 *Triturus dobrogicus*	**9.9**	**6.3**		**0.088**	**0.099**	**0.087**	**0.130**	**0.116**
4 *Triturus ivanbureschi*	0.6	**4.2**	**10.5**		**0.032**	**0.039**	**0.068**	**0.054**
5 *Triturus karelinii*	1.3	**5.0**	**11.3**	0.8		**0.043**	**0.064**	**0.052**
6 *Triturus macedonicus*	0.6	**3.1**	**9.3**	1.2	1.5		**0.080**	**0.069**
7 *Triturus marmoratus*	0.9	**4.5**	**10.8**	0.3	0.1	1.4		**0.035**
8 *Triturus pygmaeus*	**2.9**	0.7	**7.0**	**3.5**	**3.8**	2.3	**3.8**	
Correct classification	100%	100%	100%	100%	100%	100%	100%	94.1%
Idem, under cross-validation	80.0%	76.2%	71.4%	23.7%	94.1%	38.5%	66.7%	64.7.2%

Below the diagonal: differences in centroid size (CS) (absolute values × 1000). Comparisons from Tukey's honestly significant difference test for CS that were significant at the 0.05 level are shown in bold. Above the diagonal: Procrustes distances. Permutation test for Procrustes distances that were significant after Bonferroni correction are shown in bold.

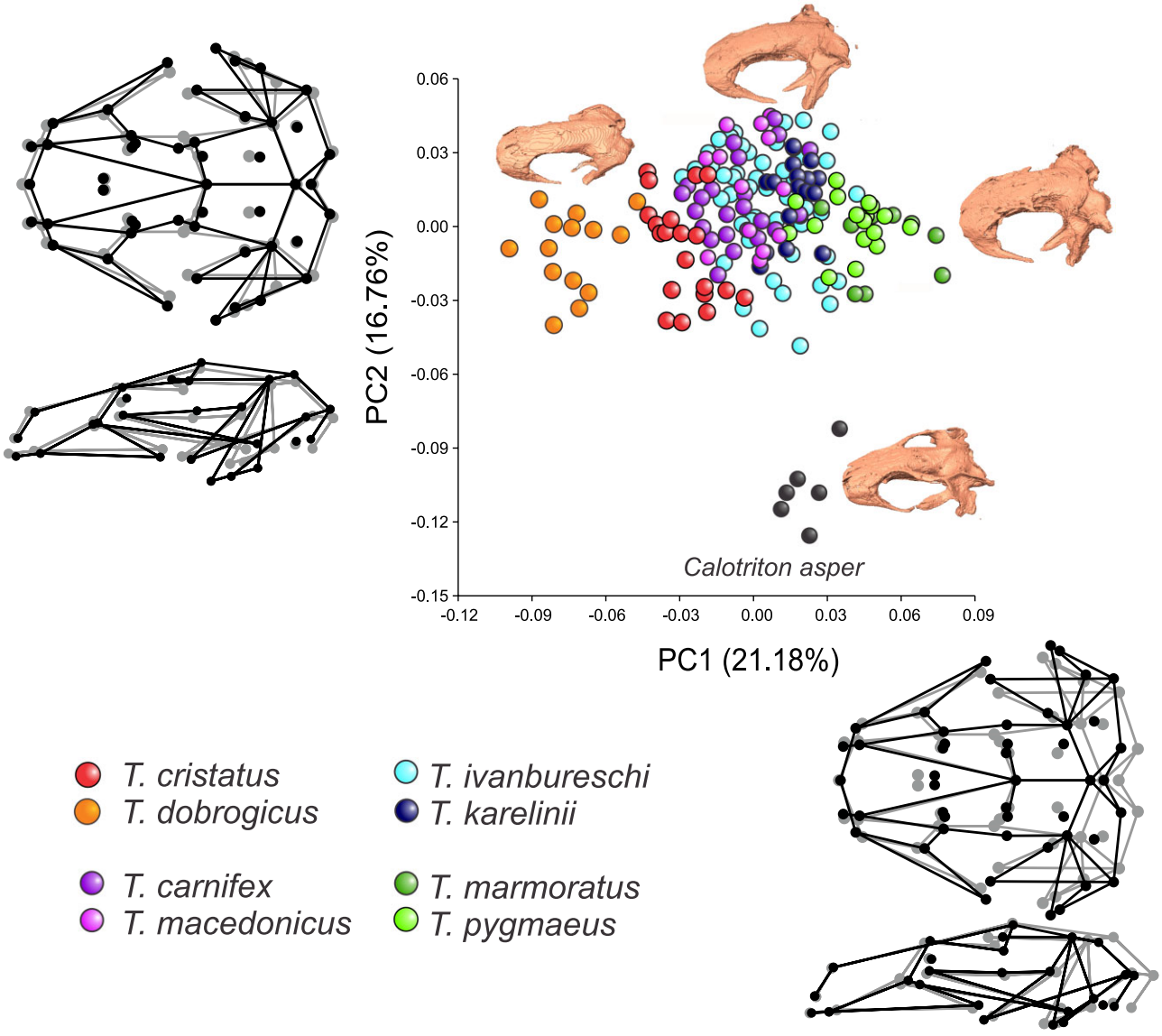

Figure 3. Position of individual newts representing eight *Triturus* species and the outgroup *Calotriton asper* over the first and second principal component axis of skull shape morphospace. Individuals with computed tomography images presented are, in clockwise order, *Triturus dobrogicus* (number 23C10), *Triturus macedonicus* (12C30), *Triturus marmoratus* (7614_167), and *C. asper* (44640). For voucher information, see Supporting information (Table S1). The observed morphological differentiation is further summarized by wireframe graphs, with the mean skull shape in grey and the shape of individual newts with maximal positive PC scores in black.

The positions of the individuals in the morphospace described by the first and second PCs are shown in Figure 3. Outgroup *C. asper* stands out as distinct and the eight *Triturus* species form a cline in morphospace, with the five aforementioned groups in the order: (1) *T. marmoratus* and *T. pygmaeus*; (2) *T. karelinii*; (3) *T. carnifex* and *T. macedonicus*; (4) *T. cristatus*; and (5) *T. dobrogicus*. Additionally, *T. ivanbureschi* from group 2 overlaps largely with group 3. A marked variation in skull shape within *T. ivanbureschi* is also suggested by the scores of correct classification (Table 1).

Marbled newts are characterized by a short otico-occipital region and, within the group, *T. marmoratus* has a slightly shorter skull base, more laterally positioned squamosals and quadrates, and relatively shorter vomeral teeth rows than has *T. pygmaeus*. Within crested newts *T. karelinii* is distinct on the

basis of: (1) a wider and shorter otico-occipital region; (2) laterally positioned squamosals and pterygoids; and (3) a well-developed snout and the shortest frontal and parietal bones. *Triturus ivanbureschi* has a similar but more variable skull shape than has *T. karelinii*. The other crested newt species have an increasingly higher skull and a more elongated and narrower otico-occipital area in order of the morphological/ecological series described above. *Triturus dobrogicus* stands apart from the other crested newt species on account of its elongated otico-occipital region, elongated parietal bones, and the more proximal position of vomerine teeth (Fig. 3).

Phylogenetic interpretation

Phylogenetic relationships incorporated in the 2D and 3D chrono-phylo-morphospace (Fig. 4) showed that marbled newts form a clearly separate cluster. Within crested newts, four species from two clades (*T. ivanbureschi–T. karelinii* and *T. carnifex–T. macedonicus*) are similar to each other and to the inferred ancestral states, suggesting a low degree of morphological differentiation (Figs 4, 5). The sister species *T. cristatus* and *T. dobrogicus* diverge in morphospace. *Triturus cristatus* shows a small shape change relative to the most recent common ancestor along with *T. carnifex* and allied species. Conversely, shape changes in the *T. dobrogicus* lineage are marked and account for most of the morphological differentiation of the genus. *Triturus dobrogicus* differs from the other species by a long skull (especially the otico-occipital region) and also by the positioning of the squamosals, quadrates, and pterygoids (Figs 3, 5).

When mapping character states over the phylogenetic tree, we found no phylogenetic signal in skull size (CS; tree length 0.001, $P > 0.05$) and significant signals in skull shape (tree length 0.021, $P < 0.05$) and body shape (NRBV; tree length 4.656, $P < 0.01$). The multivariate regression of independent contrasts of skull shape on independent contrasts of skull size revealed a significant level of evolutionary allometry ($P < 0.001$). The statistically significant regression of independent contrasts of skull shape on independent contrasts of body shape (NRBV) and independent contrasts of skull size on independent contrasts of body shape (NRBV) were found ($P < 0.001$ and $P < 0.01$, respectively).

The RV coefficient between the two hypothesized developmental modules (as derived from the neural crest versus the otico-occipital unit) is 0.88. This value is at the upper range of the distribution (either over all 3129 partitions or for 10 000 random partitions; Fig. 6), indicating high covariation among the modules.

DISCUSSION

By studying the patterns of skull size, skull shape, and body shape variation within and among eight well sampled *Triturus* species, we observed a significant association between morphological and molecular phylogenetic variation. With independent contrasts, we observed a correlated evolution of skull size, skull shape, and body shape. From the presence of a phylogenetic signal in the data, we conclude that the observed character states are in large part determined by common descent, and hence that phylogeny cannot be ignored when investigating variation among *Triturus* species.

Mapping shape character states onto the phylogeny revealed that skull evolution in *Triturus* was mostly confined to two episodes. The first episode conforms to the lineage that all crested newts have in common, namely the basal lineage that gives rise to the genus *Triturus* (node 2) toward the basal crested newt lineage (node 3) (Fig. 5). The second episode conforms to the *T. dobrogicus* lineage. In either case, the most prominent change concerns the elongation of the otico-occipital region and changes in the position of squamosal and pterygoid bones, which are positioned closer to the median plane compared to the estimated ancestral state. Shape changes that occurred from the *Triturus* MRCA (most recent common ancestor) toward the lineage that gives rise to the marbled news (node 7) concern the shortening of the otico-occipital region and the widening of the skull.

The vertebrate cranium is composed of distinct regions with different developmental pathways (Hanken & Hall, 1993), which have different functional and epigenetic interactions. These developmental and functional complexes (modules) could have independent evolutionary trajectories (Olson & Miller, 1958; Cheverud, 1995; Wagner, 1996; Klingenberg, 2008). Most studies on modularity of the vertebrate skull come from mammals (Cheverud, 1982, 1989, 1995; Marroig & Cheverud, 2001; Nicola *et al*., 2003; Zelditch & Moscarella, 2004; Monteiro & Dos Reis, 2005; Goswami, 2006a, b; Cardini & Elton, 2008a, b; Hallgrímsson *et al*., 2009) and a few other vertebrate groups (amphibians: Ivanović & Kalezić, 2010; reptiles: Monteiro & Abe, 1997; birds: Klingenberg & Marugán-Lobón, 2013). The present study showed that most of evolutionary change of *Triturus* skull concerns the otico-occipital region and contiguous skeletal elements as the squamosums and pterygoids. We hypothesized that the more or less independent changes of the otico-occipital region compared to other skull parts, reflect developmental modularity and that modularity plays an important role in the evolutionary change of skull shape in *Triturus*. Because the otico-occipital region has the

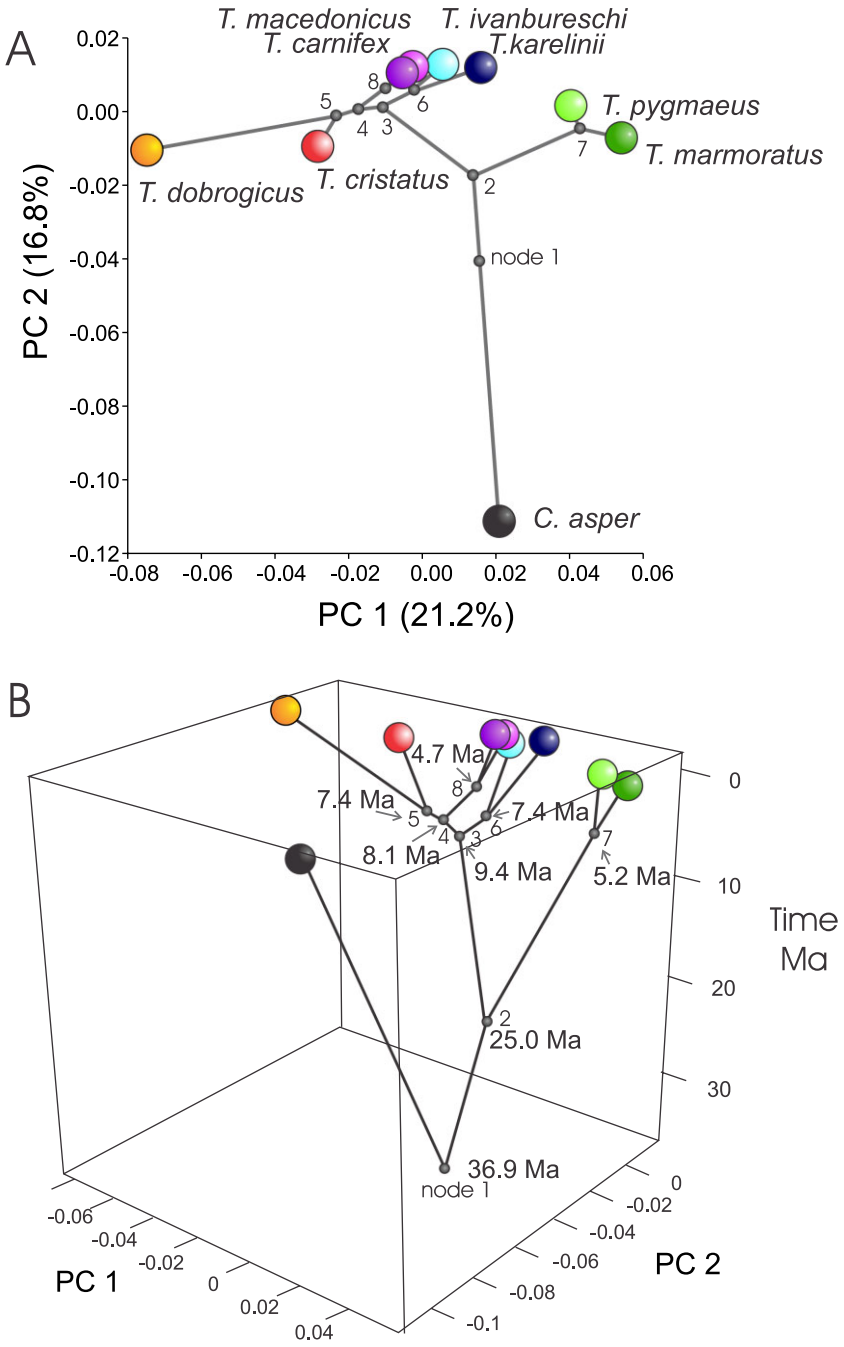

Figure 4. Position of eight *Triturus* species and the outgroup *Calotriton asper* in skull shape morphospace defined by the first and second principal component axis. A, phylo-morphospace with the species phylogeny superimposed; B, chrono-phylo-morphospace with skull shape as in (A), at the same time as showing the morphospace occupation plotted against time on the vertical axis. Internal nodes are shown by small round symbols in grey; otherwise, colour codes are as indicated in Fig. 1.

same embryonic origin as the vertebral column, we expect that constraints of a common developmental system (Richardson & Chipman, 2003) underlie coordinated change in skull shape and body shape. In other words, the selection pressures that affect somitogenesis and underlie the body elongation observed in the more aquatic *Triturus* species could also be related to a change in shape of the skull, particularly the otico-occipital unit. Our results indicate that this is not the case. Instead, both parts of

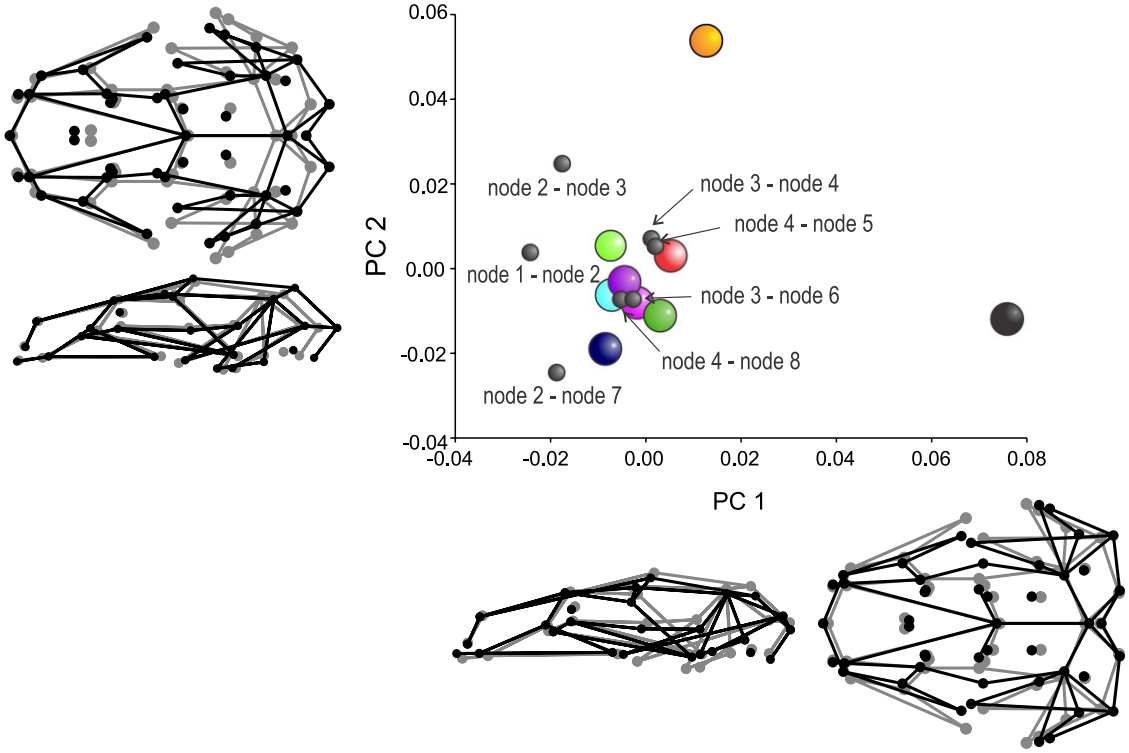

Figure 5. Summary of skull shape changes observed in the genus *Triturus*. The shape changes are shown by grey circles for internal branches and with colour coded circles for the terminal branches (colour codes are as shown in Fig. 4.). The morphological change is summarized by wireframe graphs with the mean skull shape in grey and the shape of branch with maximal principal component scores in black.

the skull evolve as one coordinated unit. This is in concordance with the results of a study on modularity and morphological integration in the related alpine newt (*Ichthyosaura alpestris*) that found a high level of integration of the newt skull, with no distinct modules (Ivanović & Kalezić, 2010).

When considering NRBV = 13 as the ancestral character state as suggested by the outgroup *C. asper*, the pattern of body shape change is one of body shortening in the marbled newt lineage (to arrive at NRBV 12) and body lengthening in crested newts (to arrive at species specific values of 13–16, with no reversals). Among the crested newts, we reconstructed a low degree of differentiation in skull shape for two groups that differ in body shape (*T. ivanbureschi–T. karelinii* group with NRBV 13 and *T.carnifex–T. macedonicus* with NRBV 14). The further body elongation in the *T. cristatus* lineage (to arrive at NRBV 15) was met with a slight change in skull shape, whereas the *T. dobrogicus* lineage (to arrive at NRBV 16 or 17) stands apart on account of an elongated otico-occipital region and a narrower skull.

The number of body segments that the vertebrate axial skeleton is composed of is determined at somitogenesis. A change in this number has major evolutionary implications as has been shown in a variety of groups (Mallo, Wellik & Deschamps, 2010). Body elongation along with reduction of limbs in tetrapods could be related to adaptations that reflect structural and functional changes associated with the switch to axial locomotion (Gans, 1975; Bajder & Hall, 2002). For salamanders, an increase in the number of segments and the body elongation that comes with it may have evolved in association with fossoriality (Jockusch, 1997), although it could also be related to a more efficient aquatic propulsion with an anguilliform swimming mode as seen in fully aquatic salamanders, such as Sirenidae and Proteidae. However, empirical work on plethodontid salamanders suggested that a relationship between body shape and microhabitat restricted to particular lineages (Jockusch, 1997; Blankers, Adams & Wiens, 2012).

In *Triturus* newts, the association of body elongation (increase in NRBV) and annual time spent in water indicates that elongated body shape is an adaptation to higher locomotory performance in aquatic environment (Arntzen & Wallis, 1999; but see also Gvoždik & Van Damme, 2006). The most extensive change of body shape is found in the *T. dobrogicus*

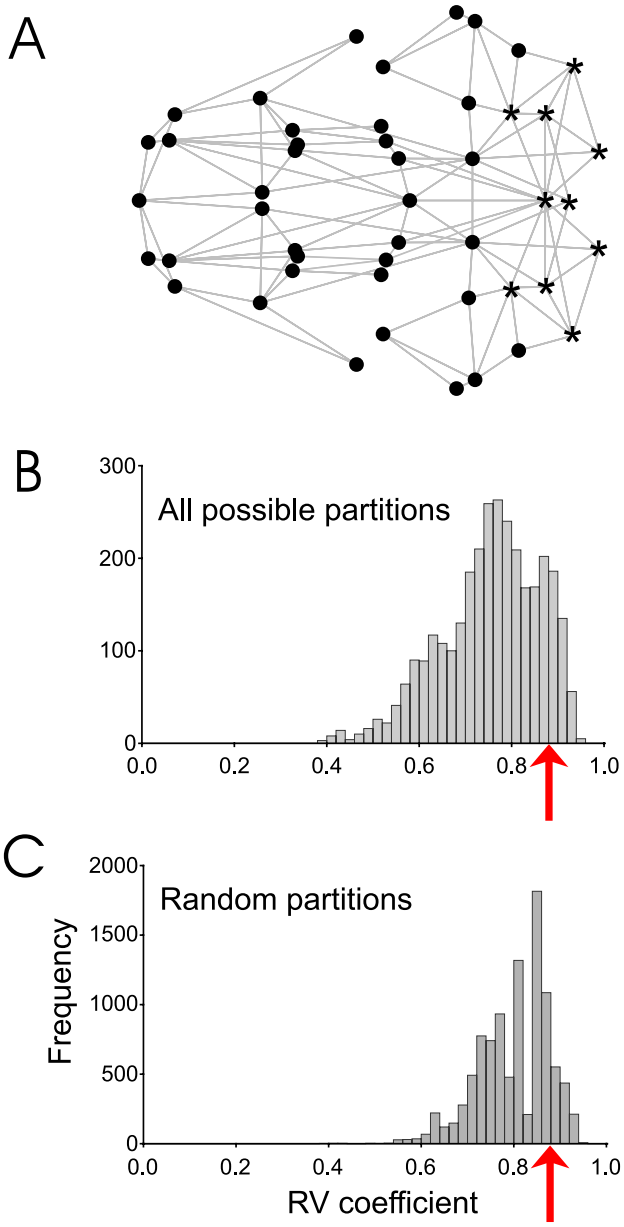

Figure 6. Modularity of the cranial skeleton as expreesed by the neural crest-derived versus otico-occipital units. A, connectivity graph defining spatially contiguous subsets of landmarks as used for testing the modularity hypothesis of the *Triturus* skull: asterisks indicate landmarks that define the otico-occipital unit; round symbols indicate landmarks that belong to the neural crest-derived module. Histograms represent the distribution of the RV coefficients for all partitions (B) and random partitions (C) of landmarks. The arrow indicates the amount of covariation (RV = 0.88) among the neural crest-derived and the otico-occipital units.

lineage. We suggest that the change may have been triggered by a niche shift towards larger and more permanent water bodies, such is presently typical for the species: extensive lowland flood plains marshes, swamps, and oxbows (Arntzen *et al*., 1997; Ivanović, Džukić & Kalezić, 2012). In line with the calibrated phylogeny of *Triturus* (see Supporting information, Fig. S1), the niche shift of *T. dobrogicus* dates back to the late Miocene (9–7.4 Mya). In this period, the Pannonian basin gradually changed from a brackish swamp to a periodically flooded delta plain (Magyar, Geary & Muller, 1999; Sacchi & Horváth, 2002; Popov *et al*., 2004).The niche that became available with the environmental transition from brackish to fresh water was taken by a lineage (eventually to become *T. dobrogicus*) that adapted to large bodies of standing water.

We consider the pattern observed in *Triturus*, in particular the association of correlated change of skull shape and body shape with niche shifts, to be a working hypothesis. We aim to test this hypothesis by enlarging our survey to include a wide representation of salamandrid salamanders.

ACKNOWLEDGEMENTS

We thank S. Litvinchuk, K. Olgun, D. Tarkhnishvili, and N. Üzüm for material; T. Vukov for help with graphical presentations; and M. Kalezić, T. Blankers, and four anonymous reviewers for their helpful comments on earlier versions of the manuscript. A.I. acknowledges financial support from the Serbian Ministry of Education and Science (grant no. 173043), a grant from SyntheSys (NL-TAF 1245, NL-TAF 3082), and an NCB Naturalis 'Temminck fellowship'.

REFERENCES

Adams DC, Nistri A. 2010. Ontogenetic convergence and evolution of foot morphology in European cave salamanders (Family: Plethodontidae). *BMC Evolutionary Biology.* **10:** 1–10.

Álvarez A, Perez SI, Verzi DH. 2013. Ecological and phylogenetic dimensions of cranial shape diversification in South American caviomorph rodents (Rodentia: Hystricomorpha). *Biological Journal Linnean Society* **110:** 898–913.

Arntzen JW. 2000. A growth curve for the newt *Triturus cristatus*. *Journal of Herpetology* **34:** 227–232.

Arntzen JW. 2003. *Triturus cristatus Superspezies* – Kammolch-Artenkreis. (*Triturus cristatus* (Laurenti, 1768) – Nördlicher Kammolch, *Triturus carnifex* (Laurenti, 1768) – Italienischer Kammolch. *Triturus dobrogicus* (Kiritzescu, 1903) – Donau-Kammolch, *Triturus karelinii* (Strauch, 1870) – Südlicher Kammolch. In: Böhme W, Grossenbacher K, eds. *Handbuch der Reptilien und Amphibien Europas*. Band 4/IIA: Schwanzlurche (Urodela) IIA. Wiebelsheim: Aula-Verlag, 421–514.

Arntzen JW, Bugter RJF, Cogalniceanu D, Wallis GP. 1997. The distribution and conservation status of the Danube crested newt, *Triturus dobrogicus*. *Amphibia-Reptilia* **18:** 133–142.

Arntzen JW, Wallis GP. 1994. The 'Wolterstorff-index' and its value in the taxonomy of the crested newt superspecies. *Abhandlungen Berichte Museum Naturkunde Vorgeschichte Magdeburg* **17:** 57–66.

Arntzen JW, Wallis GP. 1999. Geographic variation and taxonomy of crested newts (*Triturus cristatus* superspecies): morphological and mitochondrial DNA data. *Contributions to Zoology* **68:** 181–203.

Bajder L, Hall BK. 2002. Limbs in whales and limblessness in other vertebrates: mechanisms of evolutionary and developmental transformation and loss. *Evolution & Development* **4:** 445–458.

Blankers T, Adams DC, Wiens JJ. 2012. Ecological radiation with limited morphological diversification in salamanders. *Journal of Evolutionary Biology* **25:** 634–646.

Blomberg SP, Garland T, Ives AR. 2003. Testing for phylogenetic signal in comparative data: behavioral traits are more labile. *Evolution* **57:** 717–745.

Brooks DR, McLennan DA, Carpenter JM, Weller SG, Coddington JA. 1995. Systematics, ecology, and behavior: integrating phylogenetic patterns and evolutionary mechanisms. *BioScience* **10:** 687–695.

Cardini A, Elton S. 2008a. Variation in guenon skulls (I): species divergence, ecological and genetic differences. *Journal of Human Evolution* **54:** 615–637.

Cardini A, Elton S. 2008b. Does the skull carry a phylogenetic signal? Evolution and modularity in the guenons. *Biological Journal of Linnean Society* **93:** 813–834.

Cheverud JM. 1982. Phenotypic, genetic, and environmental morphological integration in the cranium. *Evolution* **36:** 499–516.

Cheverud JM. 1989. A comparative analysis of morphological variation patterns in the papionines. *Evolution* **43:** 1737–1747.

Cheverud JM. 1995. Morphological integration in the saddleback tamarin (*Saguinus fuscicollis*) cranium. *American Naturalist* **145:** 63–89.

Drummond AJ, Ho SYW, Phillips MJ, Rambaut A. 2006. Relaxed phylogenetics and dating with confidence. *PLoS Biology* **4:** e88.

Drummond AJ, Rambaut A. 2007. BEAST: Bayesian evolutionary analysis by sampling trees. *BMC Evolutionary Biology* **7:** 214.

Dryden IL, Mardia KV. 1998. *Statistical shape analysis*. New York, NY: Wiley.

Felsenstein J. 1985. Phylogenies and the comparative method. *American Naturalist* **125:** 1–15.

Galis F, Metz JAJ. 2007. Evolutionary novelties: the making and breaking of pleiotropic constraints. *Integrative and Comparative Biology* **47:** 409–419.

Gans C. 1975. Tetrapod limbless: the evolution of functional correlates. *American Zoologist* **15:** 445–467.

Goswami A. 2006a. Morphological integration in the carnivoran skull. *Evolution* **60:** 122–136.

Goswami A. 2006b. Cranial modularity shifts during mammalian evolution. *American Naturalist* **168:** 270–280.

Gould SJ. 2002. *The structure of evolutionary theory*. Cambridge, MA: Harvard University Press.

Gvoždik L, Van Damme R. 2006. *Triturus* newts defy the running-swimming dilemma. *Evolution* **60:** 2110–2121.

Hall BK. 2003. Developmental and cellular origins of the amphibian skeleton. In: Heatwole H, Davies M, eds. *Amphibian biology: osteology*, Vol. 5. Chipping Norton: Surrey Beatty & Sons, 1551–1597.

Hallgrímsson B, Jamniczky H, Young NM, Rolian C, Parsons TE, Boughner JC, Marcucio RS. 2009. Deciphering the palimpsest: studying the relationship between morphological integration and phenotypic covariation. *Evolutionary Biology* **36:** 355–376.

Hanken J, Hall BK. 1993. Mechanisms of skull diversity and evolution. In: Hanken J, Hall BK, eds. *The skull. Functional and evolutionary mechanisms*, Vol. 3. Chicago, IL: The University of Chicago Press, 1–36.

Harmon J, Weir JT, Brock CD, Glor RE, Challenger W. 2008. GEIGER: investigating evolutionary radiations. *Bioinformatics* **24:** 129–131.

Harvey PH, Pagel MD. 1991. *The comparative method in evolutionary biology*. New York, NY: Oxford University Press.

Ivanović A, Džukić G, Kalezić ML. 2012. A phenotypic point of view of the adaptive radiation of crested newts (*Triturus cristatus* superspecies, Caudata, Amphibia). *International Journal of Evolutionary Biology* **2012:** 740605.

Ivanović A, Kalezić ML. 2010. Testing the hypothesis of morphological integration on a skull of a vertebrate with a biphasic life cycle: a case study of the alpine newt. *Journal of Experimental Zoology Part B, Molecular and Developmental Evolution* **314:** 527–538.

Ivanović A, Kalezić ML. 2012. Sexual dimorphism in the skull geometry of newt species (genera *Ichthyosaura*, *Triturus* and *Lissotriton*: Caudata, Salamandridae). *Zoomorphology* **131:** 69–78.

Ivanović A, Üzüm N, Wielstra B, Olgun K, Litvinchuk SN, Kalezić ML, Arntzen JW. 2013. Is mitochondrial DNA divergence of Near Eastern crested newts (*Triturus karelinii* group) reflected by differentiation of skull shape? *Zoologischer Anzeiger* **252:** 269–277.

Jockusch EL. 1997. Geographic variation and phenotypic plasticity of number of trunk vertebrae in slender salamanders, *Batrachoseps* (Caudata: Plethodontidae). *Evolution* **51:** 1966–1982.

Klingenberg CP. 2008. Morphological integration and developmental modularity. *Annual Review of Ecology, Evolution and Systematics* **39:** 115–132.

Klingenberg CP. 2009. Morphometric integration and modularity in configurations of landmarks: tools for evaluating a-priori hypotheses. *Evolution & Development* **11:** 405–421.

Klingenberg CP. 2011. MorphoJ: an integrated software package for geometric morphometrics. *Molecular Ecology Resources* **11:** 353–357.

Klingenberg CP, Barluenga M, Meyer A. 2002. Shape analysis of symmetric structures: quantifying variation

among individuals and asymmetry. *Evolution* **56:** 1909–1920.

Klingenberg CP, Gidaszewski NA. 2010. Testing and quantifying phylogenetic signals and homoplasy in morphometric data. *Systematic Biology* **59:** 245–261.

Klingenberg CP, Marugán-Lobón J. 2013. Evolutionary covariation in geometric morphometric data: analyzing integration, modularity and allometry in a phylogenetic context. *Systematic Biology* **62:** 591–610.

Lande R, Arnold SJ. 1983. The measurement of selection on correlated characters. *Evolution* **37:** 1210–1226.

Losos JB. 2011. Seeing the forest for the trees: the limitations of phylogenies in comparative biology. *American Naturalist* **177:** 709–727.

Maddison WP. 1991. Squared-change parsimony reconstructions of ancestral states for continuous-valued characters on a phylogenetic tree. *Systematic Zoology* **40:** 304–314.

Magyar I, Geary DH, Muller P. 1999. Paleogeographic evolution of the Late Miocene Lake Pannon in Central Europe. *Palaeogeography, Palaeoclimatology, Palaeoecology* **147:** 151–167.

Mallo M, Wellik DM, Deschamps J. 2010. Hox genes and regional patterning of the vertebrate body plan. *Developmental Biology* **344:** 7–15.

Manly BFJ. 1997. *Randomization, bootstrap and Monte Carlo methods in biology*. London: Chapman & Hall.

Marroig G, Cheverud JM. 2001. A comparison of phenotypic variation and covariation patterns and therole of phylogeny, ecology and ontogeny during cranial evolution of New World monkeys. *Evolution* **55:** 2576–2600.

McArdle BH, Rodrigo AG. 1994. Estimating the ancestral states of a continuous-valued character using squared-change parsimony: an analytical solution. *Systematic Biology* **43:** 573–578.

Monteiro LR, Abe AS. 1997. Allometry and morphological integration in the skull of *Tupinambis merianae* (Lacertilia: Teiidae). *Amphibia-Reptilia* **18:** 397–405.

Monteiro LR, dos Reis SF. 2005. Morphological evolution in the mandible of spiny rats, genus *Trinomys* (Rodentia: Echimyidae). *Journal of Zoological Systematics and Evolutionary Research* **43:** 332–338.

Nicola PC, Monteiro LR, Pessôa LM, von Zuben FZ, Rohlf FJ, Dos Reis SF. 2003. Congruence of hierarchical, localized variation in cranial shape and molecular phylogenetic structure in spiny rats, genus *Trinomys* (Rodentia: Echimyidae). *Biological Journal of Linnean Society London* **80:** 385–396.

Nylander JAA. 2004. *MrModeltest*, Vol. 2. Distributed by the author. Uppsala: Uppsala University, Evolutionary Biology Centre.

Olson E, Miller R. 1958. *Morphological integration*. Chicago, IL: University Chicago Press.

Parra-Olea G, Wake DB. 2001. Extreme morphological and ecological homoplasy in tropical salamanders. *Proceedings of the National Academy of Sciences of the United States of America* **98:** 7888–7891.

Perez SI, Klaczko J, Rocatti G, dos Reis SF. 2011. Patterns of cranial shape diversification during the phylogenetic branching process of New World monkeys (Primates: Platyrrhini). *Journal of Evolutionary Biology* **24:** 1826–1835.

Popov SV, Roegl F, Rozanov AY, Steininger FF, Scherba IG, Kovač M. 2004. *Lithological–paleogeographic maps of paratethys. 10 maps late eocene to pliocene*. Frankfurt am Main: Courier Forschungsinstitut Senckenberg.

Revell LJ. 2012. PhyTools: an R package for phylogenetic comparative biology (and other things). *Methods in Ecology and Evolution* **3:** 217–223.

Richardson MK, Chipman AD. 2003. Developmental constraints in a comparative framework: a test case using variations in phalanx number during amniote evolution. *Journal of Experimental Zoology Part B, Molecular and Developmental Evolution B* **296B:** 8–22.

Rohlf FJ. 2001. Comparative methods for the analysis of continuous variables: geometric interpretations. *Evolution* **55:** 2143–2160.

Rohlf FJ, Slice D. 1990. Extensions of the procrustes method for the optimal superimposition of landmarks. *Systematic Zoology* **39:** 40–59.

Sacchi M, Horváth F. 2002. Towards a new time scale for the Upper Miocene continental series of the Pannonian basin (Central Paratethys). *European Geosciences Union Stephan Mueller Special Publication Series* **3:** 79–94.

Steinfartz S, Vicario S, Arntzen JW, Caccone A. 2007. A Bayesian approach on molecules and behavior: reconsidering phylogenetic and evolutionary patterns of the Salamandridae with emphasis on *Triturus* newts. *Journal of Experimental Zoology B* **306:** 139–162.

Wagner GP. 1996. Homologues, natural kinds and the evolution of modularity. *American Zoologist* **36:** 36–43.

Wagner GP, Mezey J. 2004. The role of genetic architecture constraints for the origin of variational modularity. In: Schlosser G, Wagner GP, eds. *Modularity in development and evolution*. Chicago, IL: Chicago University Press, 338–358.

Wake DB. 1991. Homoplasy: the result of natural selection or evidence of design limitations. *American Naturalist* **138:** 543–567.

Wielstra B, Arntzen JW. 2011. Unravelling the rapid radiation of crested newts (*Triturus cristatus* superspecies) using complete mitogenomic sequences. *BMC Evolutionary Biology* **11:** 162.

Wiens JJ, Sparreboom M, Arntzen JW. 2011. Crest evolution in newts: implications for reconstruction methods, sexual selection, phenotypic plasticity and the origin of novelties. *Journal of Evolutionary Biology* **24:** 2073–2086.

Wolterstorff W. 1923. Ubersicht der Unterarten und Formen des *Triton cristatus* Laur. *Blätter Aquar. Terrarienk. Stuttgart* **34:** 120–126.

Zelditch ML, Moscarella RA. 2004. Form, function and life history: spatial and temporal dynamics of integration. In: Pigliucci M, Preston K, eds. *Phenotypic integration*. Oxford: Oxford University Press, 274–301.

Zhang P, Papenfuss TJ, Wake MH, Qu LH, Wake DB. 2008. Phylogeny and biogeography of the family Salamandridae (Amphibia: Caudata) inferred from complete mitochondrial genomes. *Molecular Phylogenetics and Evolution* **49:** 586–597.

SUPPORTING INFORMATION

Additional Supporting Information may be found in the online version of this article at the publisher's web-site:

Figure S1. Molecular phylogeny of the newt genus *Triturus* derived from full mitogenomic sequences, reanalyzed from Wielstra & Arntzen (2011) and Wiens *et al*. (2011). The horizontal axis gives time in millions of years before present (Ma). Internal nodes are marked by number. The ages associated with nodes are given in the main text.

Table S1. The *Triturus* material included in the present study with the number of rib-bearing vertebrae (NRBV). Voucher material is in the collections of the Institute for Biological Research 'Siniša Stanković', Belgrade, Serbia (IBISS) and the Naturalis Biodiversity Center, Leiden, The Netherlands (ZMA.RenA). *N*, Number of specimens per population.

Table S2. The configuration of 48 three-dimensional landmarks identified on *Triturus* skulls. The positions of landmarks on dorsal and lateral skull are given in Fig. 2. The landmarks that belong to the subset corresponding to the otico-occipital unit are shown by asterisks.

Table S3. Summary of skull size observed in the genus *Triturus*, with mean centroid size, SD, and range.

Table S4. Principal component analysis of skull shape variables in the genus *Triturus*. Note that eigenvalues 1–23 explain over 90% of the total variation observed.